JOM, Vol. 68, No. 10, 2016
DOI: 10.1007/s11837-016-1980-4

Ultra-Fast Synthesis for Ag_2Se and CuAgSe Thermoelectric Materials

H.Z. DUAN,[1,2,3] Y.L. LI,[1,2,3] K.P. ZHAO,[1,2,3] P.F. QIU,[1,2] X. SHI,[1,2,5] and L.D. CHEN[1,2,4]

1.—State Key Laboratory of High Performance Ceramics and Superfine Microstructure, Shanghai Institute of Ceramics, Chinese Academy of Sciences, Shanghai 200050, People's Republic of China. 2.—CAS Key Laboratory of Materials for Energy Conversion, Shanghai Institute of Ceramics, Chinese Academy of Sciences, Shanghai 200050, People's Republic of China. 3.—University of Chinese Academy of Sciences, Beijing 100049, People's Republic of China. 4.—Shanghai Institute of Materials Genome, Shanghai 200050, People's Republic of China. 5.—e-mail: xshi@mail.sic.ac.cn

Ag_2Se and CuAgSe have been recently reported as promising thermoelectric materials at room temperature. The traditional melting–annealing–sintering processes are used to grow Ag_2Se and CuAgSe materials with the disadvantages of high costs of energy and time. In this work, phase-pure polycrystalline Ag_2Se and CuAgSe compounds were synthesized from raw elemental powders directly by manual mixing followed by spark plasma sintering (MM-SPS) in a few minutes. The influence of SPS heating rate on the phase composition, microstructure, and thermoelectric properties, including Seebeck coefficient, electrical conductivity, and thermal conductivity, were investigated. The zTs of 0.8 at 390 K and 0.6 at 450 K are obtained for Ag_2Se and CuAgSe, respectively, which is comparable with the values in the materials prepared by the traditional method. Furthermore, this ultrafast sample synthesis can significantly save material synthesis time and thus has the obvious advantage for large-scale production.

INTRODUCTION

Thermoelectric (TE) materials that can absorb heat in one end of the material and then transfer it to another end as heat-pumping by charge carriers have drawn great attention because of the reduction of CO_2 and greenhouse gas emissions for mitigating environmental crisis.[1–5] The performance of thermoelectric materials is evaluated by the dimensionless figure of merit zT ($zT = S^2\sigma T/\kappa$, where S is the Seebeck coefficient, σ is the electrical conductivity, T is the absolute temperature, and κ is the thermal conductivity). Good thermoelectric materials are required to possess a large Seebeck coefficient and electrical conductivity as well as a low thermal conductivity to realize high zTs.[4,6] So far, lots of advanced thermoelectric materials, such as Bi_2Te_3, PbTe, skutterudites, clathrates, Mg_2Si, Half-heusler, and Cu_2X (X=S, Se), have emerged to show high zTs above 1.0.[1,7–9] However, the commercial materials used as TE refrigerators at room temperature are only limited in Bi_2Te_3-based compounds to date. Since the elements Bi and Te are expensive and rare in the earth, it is necessary to develop other kinds of room-temperature TE materials, especially high-performance, earth-abundant, low-cost, and environmentally benign materials, for extensive industry requirements.

Recently, two kinds of new TE materials, Ag_2Se and CuAgSe, have been reported showing high thermoelectric performance around room temperature.[10–12] Ag_2Se and CuAgSe are typical "phonon-liquid electron-crystal" (PLEC) materials with ultralow lattice thermal conductivity.[8,13] Their crystal structures belong to the orthorhombic phase at room temperature, and the structures transform to superionic phase at 390 K for Ag_2Se and at 450 K for CuAgSe.[12–14] The band gaps of Ag_2Se and CuAgSe are about 0.15 eV and 0.1 eV, respectively, which is similar to that of Bi_2Te_3 (0.13 eV).[15–19] These small band gaps lead to best TE properties occurring around room temperature. For example, the reported maximum zTs of Ag_2Se and CuAgSe are about 1.0 at 400 K and 0.6 at 450 K,

(Published online June 16, 2016)

respectively, which is comparable with that of the commercial Bi_2Te_3-based compounds.[10,12] This indicates that Ag_2Se and CuAgSe are promising materials for TE application around room temperature.

Ag_2Se and CuAgSe are usually fabricated by a traditional melting–annealing–sintering process (TMAS). In the TMAS method, the samples undergo a series of complicated processes, including sealed in quartz ampules, melted at high temperatures above 1300 K, annealed for more than 1 week, and sintered for densified bulk materials by hot pressing or spark plasma sintering (SPS).[9–12,20] This traditional synthesis process causes a huge waste of time and energy and perhaps difficulty in large-scale production. Therefore, fast and economy synthesis routes are required to promote potential applications of these two new TE materials.

In this work, we occasionally find that Ag and Se powders have reactions to form Ag_2Se when mixing them together in the quartz mortar by using elements Ag and Se. Based on this interesting and abnormal phenomenon, the pure-phase Ag_2Se can be obtained by following the SPS process. More interesting, CuAgSe can also be prepared by the same process. Via this manual mixing followed by the spark plasma sintering (MM-SPS) process, we successfully fabricate phase-pure polycrystalline Ag_2Se and CuAgSe compounds. The zTs of 0.8 and 0.6 are obtained for Ag_2Se and CuAgSe, respectively, which are comparable to the TMAS samples.

EXPERIMENTAL SECTION

High-purity Cu powder (99.999%, 100 mesh, Alfa Aesar), Se powder (99.999%, 200 mesh, amorphous, Alfa Aesar), and Ag powder (99.95%, 100 mesh, Alfa Aesar) were weighed out in stoichiometric proportions of Ag_2Se and CuAgSe with the total mass around 3 g for each sample. The powders were evenly mixed by manual mixing (MM) using a mortar and pestle in the glove box for 10 min. The mixed powder was loaded into a graphite die with a diameter of 10 mm and then subjected to spark plasma sintering (SPS, Sumitomo SPS-2040). Graphite foils were placed between graphite matrices and sintered powders. The material was heated up to 673 K by using different rates such as 150 K/min, 200 K/min, and 250 K/min, and then they were kept at such temperature for 10 min under a pressure of 50 MPa. An automatic program was used for such a sintering when using the SPS. Densified bulk samples (>97% of theoretical density) with the dimensions of 10 mm in diameter and around 4 mm in thickness were obtained. The phase of the samples was determined by x-ray diffraction (XRD, D8 Advance). The morphology and elemental distribution were evaluated by scanning electron microscope (SEM, ZEISS Supra 55) and energy-dispersive x-ray (EDX, Bruker) analysis, respectively. The Seebeck coefficient and electrical conductivity were performed perpendicular to the direction of pressure by using the standard four-probe method in the ZEM-3 system (ULVAC-RIKO). The thermal diffusivity (D) was measured along the direction of pressure by using the laser flash method (Netzsch, LFA-457). The density (d) of the as-pressed sample was measured by the Archimedes method. The thermal conductivity (κ) was calculated from the relationship $\kappa = DdC_p$ by taking the Dulong-Petit value of specific heat (C_p).

RESULTS AND DISCUSSION

In the MM-SPS synthesis, we observe Ag_2Se is formed in the manual mixing process by using element Ag and Se. Then pure Ag_2Se or CuAgSe is obtained in the SPS process. Thus, the sintering processes, especially heating rate, will greatly affect the density, chemical compositions, and material microstructures as well as the TE properties,[21–23] which are listed in Table I. For all Ag_2Se and CuAgSe samples, the densities are very close to their theoretical densities.

Figure 1 shows the XRD patterns for Ag_2Se samples before and after SPS processes. Most peaks for the sample before SPS processes agree well with the standard pattern of Ag_2Se (PDF#24-1041), indicating that the main phase of Ag_2Se has formed after manual mixing. Nevertheless, Ag impurity peaks can be obviously observed, probably due to the inhomogeneity of the element distributions when mixing those powders. The Se peaks are not detected since the starting Se powder is amorphous. This indicates that Ag_2Se can be formed by hand mixing elements Ag and Se. After SPS processes, the peaks of Ag disappear and all the samples crystallize in the orthorhombic structure, which suggests that phase-pure Ag_2Se is obtained in all the samples by using different heating rates. The microstructure of Ag_2Se samples was analyzed by SEM–EDS. Elements Ag and Se are homogeneously distributed in all samples without any impurity phase or elemental agglomeration, confirming that phase-pure Ag_2Se has been prepared by MM-SPS method. Backscattered electron image and the elemental mapping for A3 are shown in Fig. 2 as an example.

Figure 3 shows the thermoelectric properties from 300 K to 390 K for all Ag_2Se samples. The reported data for TMAS samples by Mi et al.[12] are included for comparison. For all the samples prepared by MM-SPS method, the Seebeck coefficients for all samples are minus, indicating that electrons are the dominant charge carriers throughout the whole temperature range. The electrical conductivities increase and the Seebeck coefficients decrease with increasing temperature, showing a typical intrinsic semiconductor behavior. The thermal conductivities increase monotonously throughout the entire temperature range. Both electrical and thermal transport characters of the MM-SPS samples are similar to the TMAS samples.

Table I. Compositions, heating rate, and sintering temperature in the SPS sintering processes, and density for Ag_2Se and CuAgSe samples prepared by MM-SPS Method

Sample	Composition	Heating rate (K/min)	Sintering temperature (K)	Density (g/cm^3)
A1	Ag_2Se	150	673	8.28
A2	Ag_2Se	200	673	8.22
A3	Ag_2Se	250	673	8.21
B1	CuAgSe	150	673	7.78
B2	CuAgSe	200	673	7.73
B3	CuAgSe	250	673	7.72

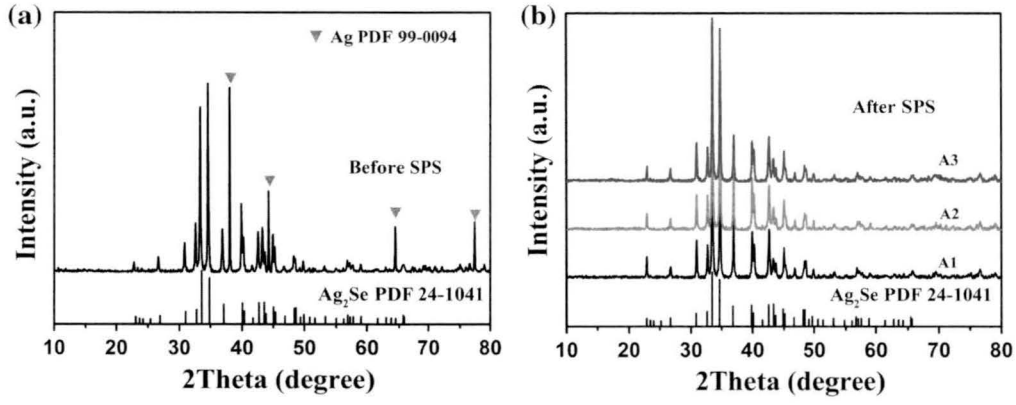

Fig. 1. Powder XRD patterns for Ag_2Se (a) before SPS process and (b) after SPS process by using different heating rates.

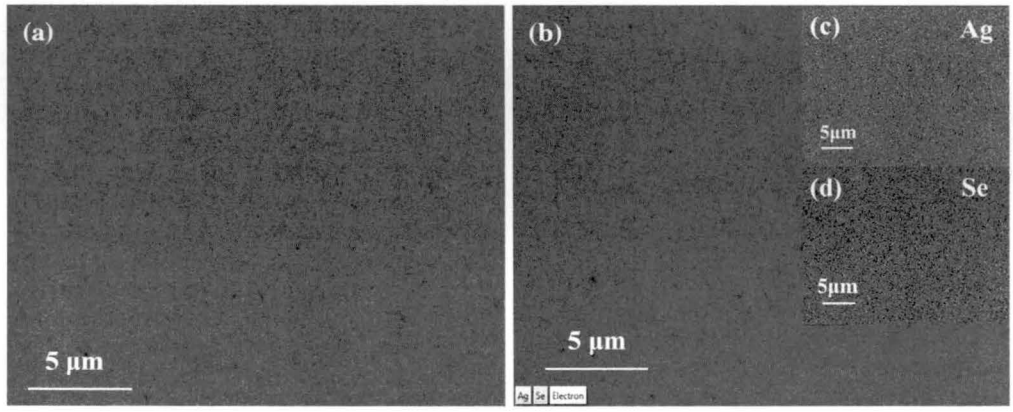

Fig. 2. Scanning electron microscopy (SEM) images of A3: (a) backscattered electron image, and elemental mappings of (b) all elements, (c) Ag, and (d) Se.

Nevertheless, the values of electrical and thermal properties show a deviation for the MM-SPS samples by using different heating rates. For example, sample A1 shows the largest electrical and thermal conductivities with the values similar to the TMAS Ag_2Se by Mi et al.[12] Sample A2 shows the lowered electrical and thermal conductivities, which are close to that of $Ag_2Se_{1.08}$ in Ref. [12]. The possible reason is that the atomic ratio of Ag and Se may slightly deviate from the stoichiometric ratio in the SPS sintering processes when using different heating rates. The consistent electrical and thermal transport properties with TMAS samples lead to the similar zT values for the MM-SPS samples. The highest zT of about 0.8 at 390 K is obtained in sample A2.

The XRD patterns for CuAgSe prepared by MM-SPS method are plotted in Fig. 4. Similar to the situation of Ag_2Se, the Ag_2Se phase has formed by manual mixing. It can be obviously observed in the XRD pattern of the manual mixed powder before SPS process (see Fig. 4a). Figure 4b displays the

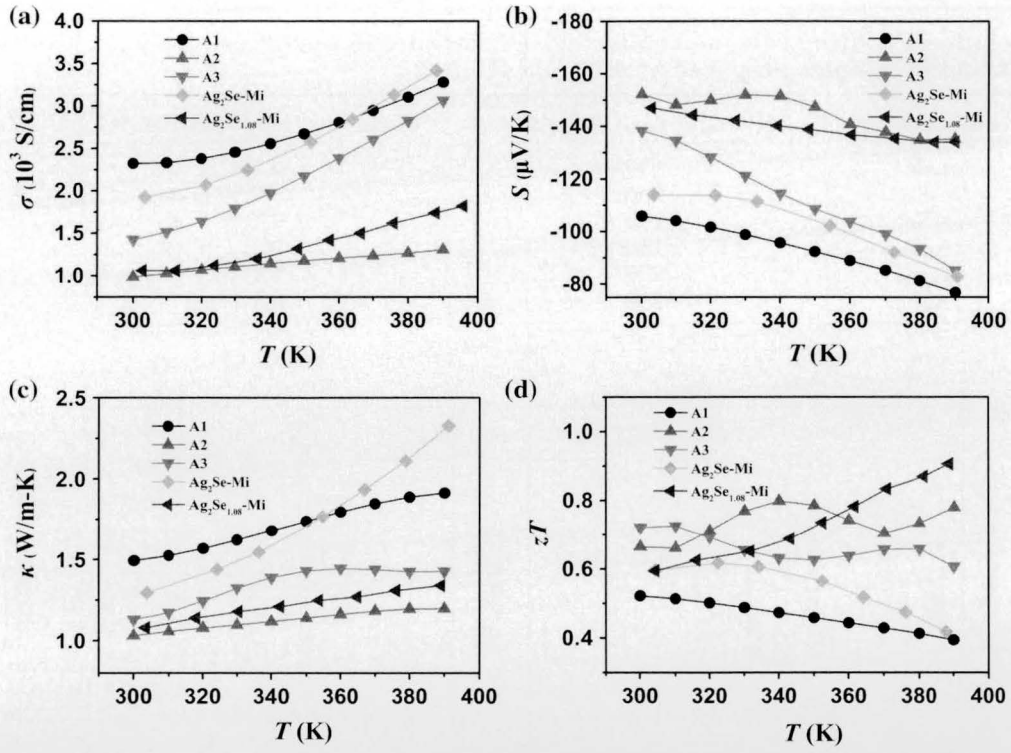

Fig. 3. Thermoelectric properties of Ag_2Se. (a) Temperature-dependent electrical conductivity σ, (b) Seebeck coefficient S, (c) thermal conductivity κ, and (d) thermoelectric figure of the merit zT for Ag_2Se prepared by MM-SPS method with the heating rates of 150 K/min, 200 K/min, and 250 K/min. The reported data for TMAS samples by Mi[12] are included for comparison.

XRD patterns of the samples after SPS sintering by using different heating rates. For all the samples, the main peaks are consistent with the standard patterns PDF#10-0451 (orthorhombic CuAgSe) and PDF#25-1180 (tetragonal CuAgSe). This is in agreement with the previous studies.[10,16] Some impurity diffraction peaks around 34°, which are identified as belonging to Ag_2Se phase, are observed in the XRD pattern of sample B1.

The microstructure analysis by SEM is presented in Fig. 5. The CuAgSe samples with different heating rates show different microstructures. For sample B1 and B2 with low heating rates, the bright impurity areas are clearly observed, as shown in Fig. 5a and b. These impurity phases are identified as Ag_2Se by SEM–EDS, which is consistent with the XRD result. When increasing the heating rate, the amount of Ag_2Se decreases gradually. For sample B3 with a heating rate of 250 K/min, the impurity phase disappears completely (see Fig. 5c). In the elemental x-ray mapping of B3 by EDS, elements Cu, Ag, and Se are all homogeneously distributed in the sample and no impurity phases are detected. This indicates that homogeneous and phase-pure CuAgSe compound is obtained by the MM-SPS method under the heating rate of 250 K/min.

The thermoelectric properties from room temperature to 450 K for CuAgSe samples prepared by MM-SPS method with different heating rates are shown in Fig. 6. The reported data for the CuAgSe sample prepared by TMAS method are included for comparison. For sample B3, the values and the temperature dependences of electrical conductivity and Seebeck coefficient are in good agreement with that of the TMAS samples. Nevertheless, for samples B1 and B2 that have some impurity phases (see Fig. 5a and b), both electrical conductivity and the Seebeck coefficient deviate from the value of phase-pure CuAgSe since the impurities can greatly change the TE properties.[10] Figure 6c shows the thermal conductivity for CuAgSe samples from room temperature to 450 K. The thermal conductivity of all samples decreases monotonously throughout the entire temperature range, which is similar to that of the TMAS sample. The lowest thermal conductivity for B3 is about 1.1 W m^{-1} K^{-1} at 450 K. The dimensionless thermoelectric figure of merit zT for all samples is shown in Fig. 6d. For the phase-pure CuAgSe (sample B3), it shows almost the same zT values with TMAS sample throughout the whole temperature range. The maximum zT around 0.6 at 450 K is observed.

To explore the role of the SPS process in the formation of a phase-pure CuAgSe compound, we measured the change of material's chemical compositions during the entire course of the SPS process by using SEM. Three samples with the same initial powders are heated up to three different temperatures (350 K, 470 K, and 670 K) with a heating rate of 250 K/min and then cooled immediately to room

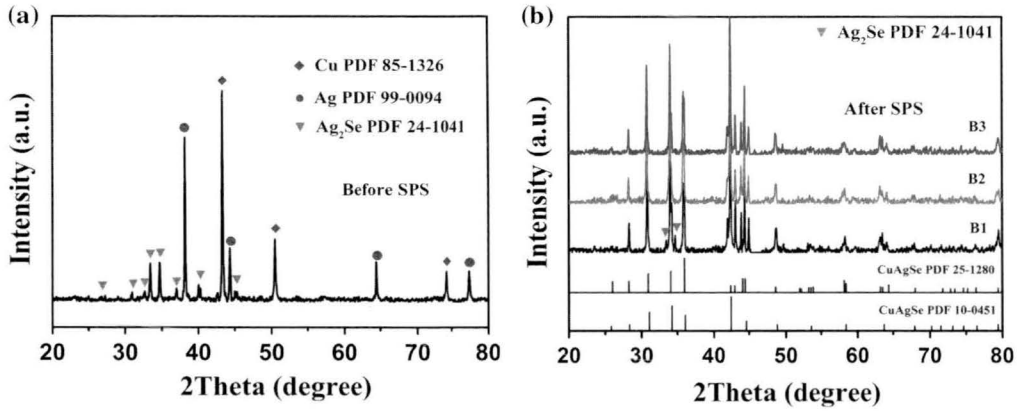

Fig. 4. Powder XRD patterns for CuAgSe (a) before SPS process and (b) after SPS process by using different heating rates.

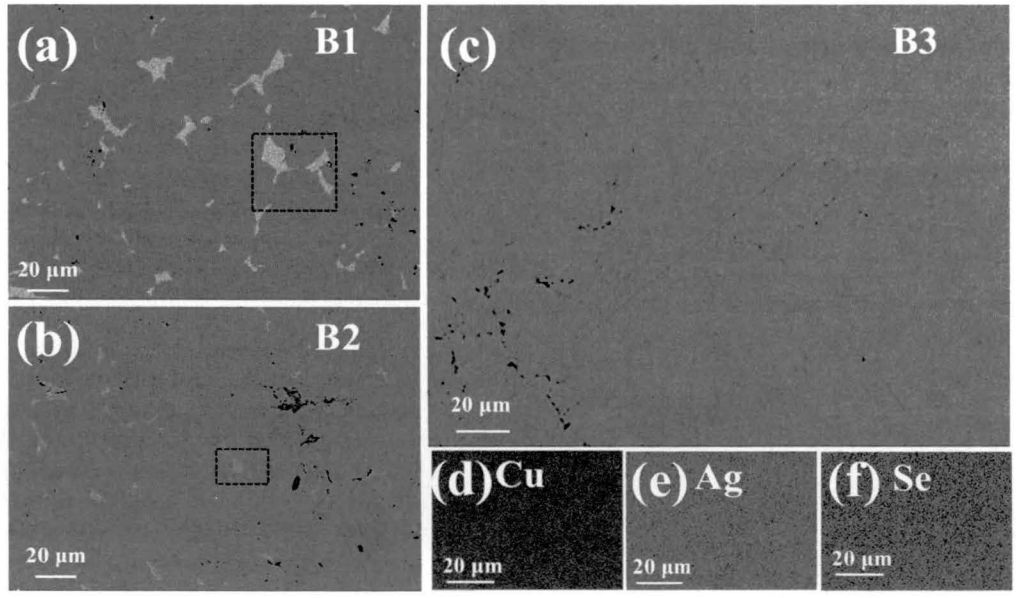

Fig. 5. Backscattered electron images for the samples (a) B1, (b) B2, and (c) B3 synthesized by MM-SPS method and elemental mappings of (d) Cu, (e) Ag, and (f) Se for sample B3.

temperature. The elemental mappings of these three samples frozen at designed temperatures are shown in Fig. 7. When the designed temperature is at 350 K, the sample is a mixture of Ag_2Se, CuSe, and elemental Cu, which is close to the case of mixed powders where Ag_2Se and elemental Cu, Ag, and Se are observed (see Figs. 7a and 4a) with a relatively low density of 6.50 g/cm^3. This indicates that the chemical reaction has just begun at 350 K. When temperatures increase, the amount of impurity phases decreases gradually and the amount of CuAgSe phase increases (see Fig. 7b), leading to an increased density up to 7.60 g/cm^3. When the designed temperature is at 670 K, pure CuAgSe with a high density of 7.75 g/cm^3 is obtained without impurity phases observed (see Fig. 7c). The evolution of the phase compositions at different sintering temperatures during the SPS processes implies that the function of SPS is to promote element diffusions and chemical reactions to form phase-pure CuAgSe.

CONCLUSION

In this article, Ag_2Se and CuAgSe room-temperature thermoelectric materials have been successfully synthesized by manual mixing followed by spark plasma sintering (MM-SPS). Ag_2Se phase is formed directly in the manual mixing process. The single-phase Ag_2Se and CuAgSe compounds with more than 97% of theoretical density are obtained by the subsequent SPS processes. The XRD results, backscattered electron images, and elemental mappings prove that the samples prepared by the MM-SPS method possess pure phases and homogenous compositions. The thermoelectric

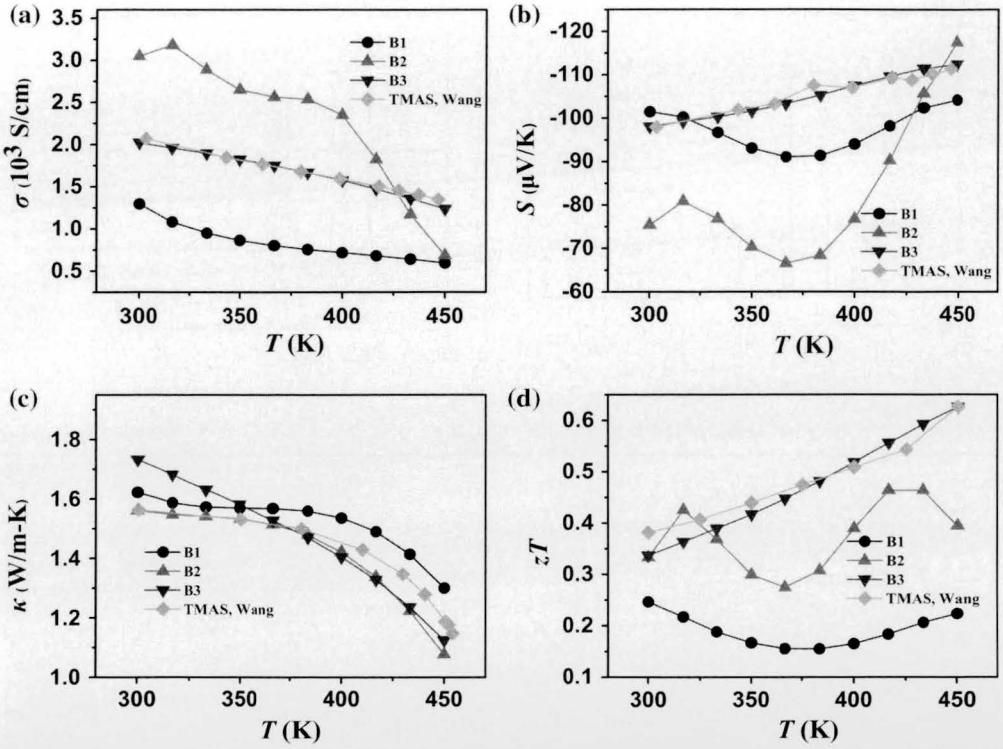

Fig. 6. Thermoelectric properties of CuAgSe. (a) Temperature-dependent electrical resistivity σ, (b) Seebeck coefficient S, (c) thermal conductivity κ, and (d) thermoelectric figure of the merit zT for CuAgSe prepared by MM-SPS method with heating rates of 150 K/min, 200 K/min, and 250 K/min. The reported data for TMAS sample by Wang[10] are included for comparison.

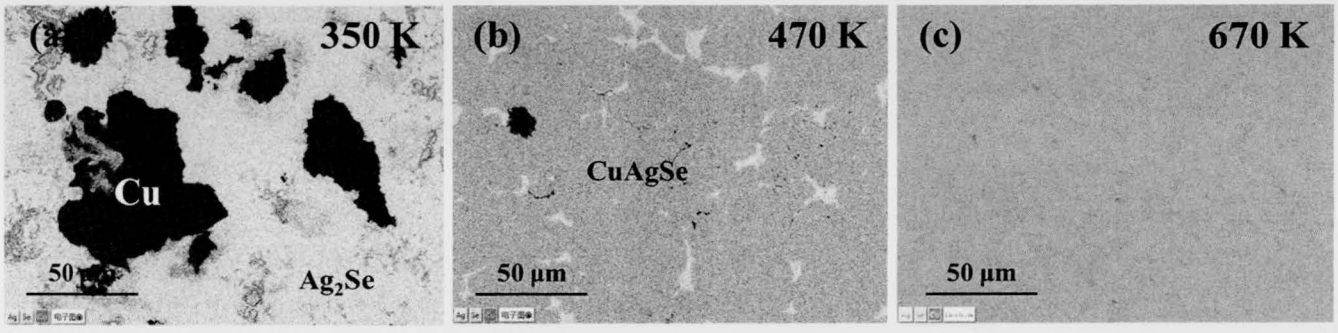

Fig. 7. Elemental mappings for the samples frozen at (a) 350 K, (b) 470 K, and (c) 670 K.

properties of the MM-SPS samples are consistent with that of TMAS samples. The maximum zTs of 0.8 at 390 K for Ag_2Se and 0.6 at 450 K for CuAgSe are obtained, which is comparable to the TMAS samples. As compared with the conventional method, this fast and economic method has the potential to promote the large-scale fabrication of Ag_2Se- and CuAgSe-based thermoelectric materials. To help the future experiments, we can give some suggestions from our experience: (I) Binary compounds are easily fabricated; (II) A fast heating rate is helpful for obtaining phase-pure materials, but a too fast heating rate may melt the samples. For CuAgSe and Ag_2Se compounds, the heating rate should be less than 300 K/min.

ACKNOWLEDGEMENTS

This work is supported by the National Basic Research Program of China (973-Program) under Project No. 2013CB632501, the National Natural Science Foundation of China (NSFC) under the No. 51472262 and 51402337, the Key Research Program of Chinese Academy of Sciences (Grant No. KGZD-EW-T06), and International S&T Cooperation Program of China (2015DFA51050).

REFERENCES

1. G.J. Snyder and E.S. Toberer, *Nat. Mater.* 7, 105 (2008).
2. L.E. Bell, *Science* 321, 1457 (2008).
3. F.J. DiSalvo, *Science* 285, 703 (1999).
4. K. Ono and R.O. Suzuki, *J. Miner. Met. Mater. Soc.* 50, 48 (1998).
5. L.D. Chen, Z. Xiong, and S.Q. Bai, *J. Inorg. Mater.* 25, 561 (2010).
6. K. Biswas, J. He, I.D. Blum, C.I. Wu, T.P. Hogan, D.N. Seidman, V.P. Dravid, and M.G. Kanatzidis, *Nature* 489, 414 (2012).
7. W. Liu, K.C. Lukas, K. McEnaney, S. Lee, Q. Zhang, C.P. Opeil, G. Chen, and Z. Ren, *Energy Environ. Sci.* 6, 552 (2013).
8. H.L. Liu, X. Shi, F.F. Xu, L.L. Zhang, W.Q. Zhang, L.D. Chen, Q. Li, C. Uher, T. Day and G.J. Snyder, *Nat. Mater.* 11, 422 (2012).
9. X. Shi, J. Yang, J.R. Salvador, M.F. Chi, J.Y. Cho, H. Wang, S.Q. Bai, J.H. Yang, W.Q. Zhang, and L.D. Chen, *J. Am. Chem. Soc.* 133, 7837 (2011).
10. X.B. Wang, P.F. Qiu, T.S. Zhang, D.D. Ren, L.H. Wu, X. Shi, J.H. Yang, and L.D. Chen, *J. Mater. Chem. A* 3, 13662 (2015).
11. P.F. Qiu, X.B. Wang, T.S. Zhang, X. Shi, and L.D. Chen, *J. Mater. Chem. A* 3, 22454 (2015).
12. W.L. Mi, P.F. Qiu, T.S. Zhang, Y.H. Lv, X. Shi, and L.D. Chen, *Appl. Phys. Lett.* 104, 133903 (2014).
13. H.L. Liu, X. Yuan, P. Lu, X. Shi, F.F. Xu, Y. He, Y.S. Tang, S.Q. Bai, W.Q. Zhang, L.D. Chen, Y. Lin, L. Shi, H. Lin, X.Y. Gao, X.M. Zhang, H. Chi, and C. Uher, *Adv. Mater.* 25, 6607 (2013).
14. A.J. Hong, T. Li, H.X. Zhu, X.H. Zhou, Q.Y. He, W.S. Liu, Z.B. Yan, J.M. Liu, and Z.F. Ren, *Solid State Ionics* 261, 21 (2014).
15. L.P. Hu, T.J. Zhu, Y.G. Wang, H.H. Xie, Z.J. Xu, and X.B. Zhao, *NPG Asia Mater.* 6, e88 (2014).
16. C. Han, Q. Sun, Z.X. Cheng, J.L. Wang, Z. Li, G.Q. Lu, and S.X. Dou, *J. Am. Chem. Soc.* 136, 17626 (2014).
17. H.F. Wang, W.G. Chu, D.W. Wang, W.C. Mao, W.Z. Pan, Y.J. Guo, Y.F. Xiong, and H. Jin, *J. Electron. Mater.* 40, 624 (2011).
18. C. Lee, Y.H. Park, and H. Hashimoto, *J. Appl. Phys.* 101, 024920 (2007).
19. C.M. Fang, R.A. de Groot, and G.A. Wiegers, *J. Phys. Chem. Solids* 63, 457 (2002).
20. Y.T. Qiu, J.J. Xing, X. Gao, L.L. Xi, X. Shi, H. Gu, and L.D. Chen, *J. Mater. Chem. A* 2, 10952 (2014).
21. A.B. Blichfeld and B.B. Iversen, *J. Mater. Chem. C* 3, 10543 (2015).
22. H. Yin, A.B. Blichfeld, M. Christensen, B.B. Iversen, and A.C.S. Appl, *Mater. Interfaces* 6, 10542 (2014).
23. Z.A. Munir, U. Anselmi-Tamburini, and M. Ohyanagi, *J. Mater. Sci.* 41, 763 (2006).